Conversion of Sugars to Lactic Acid Derivatives Using Heterogeneous Zeotype Catalysts

Martin Spangsberg Holm, *et al.*

Science **328**, 602 (2010);
DOI: 10.1126/science.1183990

2% (*8*). However, they constitute a significant fraction of the supermassive black hole mass density in the universe (*29*). Adding the extra obscured accretion reported here, which lasts as long as the optically bright phase, increases our original estimate of the integrated black hole mass density at $z = 0$ by 4%, to $4.5 \times 10^5\ M_\odot\ \mathrm{Mpc}^{-3}$ (*8*). Including this additional contribution, the integrated black hole growth in the obscured quasar phase is $1.3 \times 10^5\ M_\odot\ \mathrm{Mpc}^{-3}$, or ~ 30% of the total black hole mass density at $z = 0$, in agreement with our conclusion that the obscured quasar phase can harbor a large fraction of the black hole growth (*30*). Our results are in agreement with recent estimates (*26*) that suggest an average accretion efficiency of ≤10% even accounting for heavily obscured accretion.

References and Notes

1. By quasar, we refer here to the most luminous members of the AGN family, typically $M_B < -23$, $L_X > 10^{44}$ erg/s or $L_{bol} > 10^{45}$ erg/s.
2. M. Schmidt, *Nature* **197**, 1040 (1963).
3. G. T. Richards *et al.*, *Astrophys. J.* **180** (suppl.), 67 (2009).
4. A. J. Barger *et al.*, *Astron. J.* **126**, 632 (2003).
5. N. L. Zakamska *et al.*, *Astron. J.* **126**, 2125 (2003).
6. A. Martínez-Sansigre *et al.*, *Mon. Not. R. Astron. Soc.* **370**, 1479 (2006).
7. R. Gilli, M. Salvati, G. Hasinger, *Astron. Astrophys.* **366**, 407 (2001).
8. E. Treister, C. M. Urry, S. Virani, *Astrophys. J.* **696**, 110 (2009).
9. D. B. Sanders *et al.*, *Astrophys. J.* **325**, 74 (1988).
10. D. B. Sanders, I. F. Mirabel, *Annu. Rev. Astron. Astrophys.* **34**, 749 (1996).
11. J. E. Barnes, L. E. Hernquist, *Astrophys. J.* **370**, L65 (1991).
12. R. Genzel *et al.*, *Astrophys. J.* **498**, 579 (1998).
13. By heavily obscured, we refer here to sources with neutral hydrogen column densities $N_H > 10^{23}\ \mathrm{cm}^{-2}$, enough to hide most of the soft x-rays to optical quasar signatures.
14. P. Tozzi *et al.*, *Astron. Astrophys.* **451**, 457 (2006).
15. D. M. Alexander *et al.*, *Astrophys. J.* **687**, 835 (2008).
16. F. Fiore *et al.*, *Astrophys. J.* **693**, 447 (2009).
17. E. Treister *et al.*, *Astrophys. J.* **706**, 535 (2009).
18. D.-C. Kim, D. B. Sanders, *Astrophys. J.* **119** (suppl.), 41 (1998).
19. P. F. Hopkins, L. Hernquist, T. J. Cox, D. Keres, *Astrophys. J.* **175** (suppl.), 356 (2008).
20. P. F. Hopkins *et al.*, http://arxiv.org/abs/0906.5357 (2009).
21. D. Marchesini *et al.*, *Astrophys. J.* **701**, 1765 (2009).
22. T. Dahlen *et al.*, *Astrophys. J.* **654**, 172 (2007).
23. G. Hasinger, T. Miyaji, M. Schmidt, *Astron. Astrophys.* **441**, 417 (2005).
24. A. J. Barger *et al.*, *Astron. J.* **129**, 578 (2005).
25. G. T. Richards *et al.*, *Astron. J.* **131**, 2766 (2006).
26. A. Martínez-Sansigre, A. M. Taylor, *Astrophys. J.* **692**, 964 (2009).
27. M. Dietrich, S. Mathur, D. Grupe, S. Komossa, *Astrophys. J.* **696**, 1998 (2009).
28. M. Vestergaard, P. S. Osmer, *Astrophys. J.* **699**, 800 (2009).
29. M. G. Haehnelt, P. Natarajan, M. J. Rees, *Mon. Not. R. Astron. Soc.* **300**, 817 (1998).
30. This integrated value was obtained assuming an accretion efficiency of 0.1 and is in very good agreement with observational results (*31*), even after incorporating this additional accretion.
31. A. Marconi *et al.*, *Mon. Not. R. Astron. Soc.* **351**, 169 (2004).
32. R. Della Ceca *et al.*, *Astron. Astrophys.* **487**, 119 (2008).
33. S. H. Teng *et al.*, *Astrophys. J.* **691**, 261 (2009).

34. Support for the work of E.T. and K.S. was provided by the National Aeronautics and Space Administration (NASA) through Chandra/Einstein Postdoctoral Fellowship award numbers PF8-90055 and PF9-00069, respectively, issued by the Chandra X-ray Observatory Center, which is operated by the Smithsonian Astrophysical Observatory for and on behalf of NASA under contract NAS8-03060. P.N. acknowledges the Radcliffe Institute for Advanced Study where this work was started. C.M.U. acknowledges support from NSF grant AST-0407295.

Supporting Online Material

www.sciencemag.org/cgi/content/full/science.1184246/DC1
SOM Text
Figs. S1 and S2
References

4 November 2009; accepted 17 March 2010
Published online 25 March 2010;
10.1126/science.1184246
Include this information when citing this paper.

Conversion of Sugars to Lactic Acid Derivatives Using Heterogeneous Zeotype Catalysts

Martin Spangsberg Holm,[1,2,3]* Shunmugavel Saravanamurugan,[1,2]* Esben Taarning[2,3]†

Presently, very few compounds of commercial interest are directly accessible from carbohydrates by using nonfermentive approaches. We describe here a catalytic process for the direct formation of methyl lactate from common sugars. Lewis acidic zeotypes, such as Sn-Beta, catalyze the conversion of mono- and disaccharides that are dissolved in methanol to methyl lactate at 160°C. With sucrose as the substrate, methyl lactate yield reaches 68%, and the heterogeneous catalyst can be easily recovered by filtration and reused multiple times after calcination without any substantial change in the product selectivity.

Carbohydrates represent the largest fraction of biomass, and various strategies for their efficient use as a commercial chemical feedstock are being established in the interest of supplementing, and ultimately replacing, petroleum (*1*–*4*). The thermal instability of carbohydrates is a major obstacle in this regard, and biochemical processes have proven to be more applicable than catalytic ones, in part because of their ability to operate at low temperatures. On the other hand, catalysis often presents improved process design options, resulting in higher productivity and reduced costs related to product work-up. Indeed, catalysis has proven to be scalable and able to supply numerous low-cost products from petroleum.

In contrast to the case for biochemical processes, relatively few products are directly obtainable from carbohydrates by using catalysis. Gluconic acid and sorbitol can be obtained from glucose by oxidation and hydrogenation, respectively, and acidic catalysts are currently being examined for the direct production of 5-hydroxymethylfurfural (HMF) (*5*–*7*). However, currently the production of fuels and value-added compounds from carbohydrates is dominated by fermentative processes (*8*). An important example is the fermentation of glucose to lactic acid, which is used for the production of biodegradable plastics (*9*, *10*) and solvents (*11*, *12*). Lactic acid has also been investigated as a precursor to the production of a wide range of useful compounds through catalytic transformation (*13*, *14*). However, the future role of lactic acid will largely depend on its production costs. Because the fermentation of glucose to lactic acid

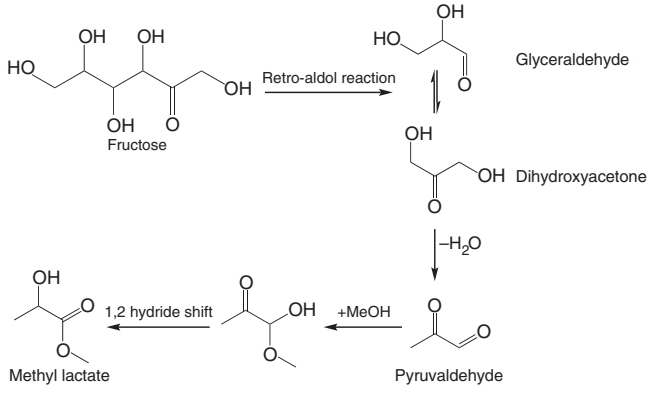

Fig. 1. Proposed reaction pathway for the conversion of fructose to methyl lactate. The reaction formally comprises a retro aldol fragmentation of fructose and isomerization-esterification of the trioses.

[1]Centre for Catalysis and Sustainable Chemistry, Department of Chemistry, Technical University of Denmark, Anker Engelundsvej 1, 2800 Kongens Lyngby, Denmark. [2]Center for Sustainable and Green Chemistry, Department of Chemistry, Technical University of Denmark, Anker Engelundsvej 1, 2800 Kongens Lyngby, Denmark. [3]Haldor Topsøe A/S, Nymøllevej 55, 2800 Kongens Lyngby, Denmark.

*These authors contributed equally to this work.
†To whom correspondence should be addressed. E-mail: esta@topsoe.dk

involves the coproduction of large amounts of salt waste, a less expensive route would be an important step toward a biomass-based chemical industry using lactic acid more widely as a feedstock. Here we show that sucrose, glucose, and fructose dissolved in methanol can be converted directly into racemic methyl lactate in yields up to 68% in a process resembling the alkaline degradation of sugars. Methyl lactate can be purified by distillation, and its one-pot formation offers an advantage over the fermentative route, wherein the esterification of lactic acid to methyl lactate is often necessary.

We recently reported that Lewis acidic zeolites and zeotypes efficiently catalyze the conversion, in methanol, of the two trioses dihydroxyacetone and glyceraldehyde to methyl lactate at moderate temperatures (*15*, *16*). Here we report that while investigating the properties of the Sn-Beta zeolite for fructose transformation, we discovered that, at elevated temperatures, fructose is transformed to methyl lactate in yields of up to 44%. We assume that this reaction proceeds via a retro aldol reaction of fructose forming two trioses (Fig. 1). These trioses are readily converted to the thermodynamically very stable methyl lactate through sequential dehydration and methanol addition, followed by a 1,2-hydride shift as reported previously (*15*–*17*). Indeed, at intermediate reaction times, small amounts of unconverted triose sugars were observed by high-performance liquid chromatography (HPLC), supporting the existence of this reaction pathway.

A retro aldol reaction is favored at high temperatures, and fructose and glucose are known to undergo fragmentation in supercritical water to form C_2 to C_4 carbohydrate products (*18*, *19*). In the presence of aqueous alkali hydroxides, the transformation of the monosaccharides to lactate salts occurs at milder conditions (100° to 260°C) (*20*–*22*). However, to obtain high lactate yields, a stoichiometric amount of base is required because of the acid-base reaction between lactic acid and hydroxide. For the Sn-Beta–catalyzed reaction in methanol, we observed methyl lactate formation from fructose at temperatures as low as 140°C. This observation suggests that the retro aldol reaction is the rate-determining step in the overall transformation of fructose, because methyl lactate is readily formed from trioses at lower temperatures (80°C) (*15*). Glucose and sucrose are less expensive and much more abundant sugars than fructose, and therefore these substrates were also investigated for the production of methyl lactate.

We have synthesized highly crystalline Beta zeolites and zeotypes with the BEA framework topology that differ in the type of metal that is incorporated into the framework according to established procedures (*23*). They can be divided into Lewis acidic (Ti-, Sn-, and Zr-Beta), Brønsted acidic (H-Al-Beta), and nonacidic (Si-Beta) classes. These materials contain well-defined metal single sites that were found to have catalytic activity in various reactions (*24*–*26*). Zeolite Beta has a three-dimensional porous system with 12-ring pores that are sufficiently large to accommodate acyclic monosaccharides (*27*). We tested these materials for the conversion of sugars at 160°C in an autoclave setup (Table 1).

In agreement with previous reports (*28*), we found that the Brønsted acidic zeolite H-Al-Beta catalyzes the dehydration of the sugars, leading to HMF derivatives and methyl levulinate from fructose and predominantly methyl-D-pyranoside from glucose and sucrose (table S1). The Lewis acidic zeolites, on the other hand, were found to induce high selectivities toward methyl lactate. Sn-Beta is the most selective, giving a methyl lactate yield of 64 to 68%, which was calculated on a carbon basis when using sucrose as the substrate. Of the three Lewis acidic zeolites, Sn-Beta has the strongest Lewis acidic sites, which could explain its higher selectivity (*15*, *29*). However, both Zr-Beta and Ti-Beta are capable of producing methyl lactate in moderate yields (31 to 44%). The nonacidic Si-Beta did not improve the yield of methyl lactate over that of the background reaction, indicating that the catalytic ability is related to the Lewis acidity of

Table 1. Conversion of sugars using different zeolite and zeotype materials. Substrate (225 mg), catalyst (160 mg), naphtalene (120 mg), and methanol (8.0 g) were stirred in an autoclave at 160°C for 20 hours. Yields are calculated on a carbon basis and given as mean values. The key experiments converting sucrose using Ti-, Zr-, and Sn-Beta were repeated five times (see table S5 for statistical information). Conversion is calculated based on the amount of unconverted hexoses. Si/M, Si/metal ratio in the synthesis gel.

Catalyst	Si/M	Substrate	Conversion	Yield of methyl lactate
H-(Al)-Beta	125	Glucose	97%	0%
H-(Al)-Beta	125	Fructose	>99%	1%
H-(Al)-Beta	125	Sucrose	99%	0%
Ti-Beta	125	Glucose	99%	31%
Ti-Beta	125	Fructose	>99%	36%
Ti-Beta	125	Sucrose	98%	44%
Zr-Beta	125	Glucose	99%	33%
Zr-Beta	125	Fructose	>99%	33%
Zr-Beta	125	Sucrose	99%	40%
Sn-Beta	125	Glucose	>99%	43%
Sn-Beta	125	Fructose	>99%	44%
Sn-Beta	125	Sucrose	>99%	64%
Si-Beta	—	Glucose	61%	5%
Si-Beta	—	Fructose	79%	9%
Si-Beta	—	Sucrose	63%	6%
No catalyst	—	Glucose	53%	5%
No catalyst	—	Fructose	67%	8%
No catalyst	—	Sucrose	54%	6%
$SnCl_4 \cdot 5H_2O$*	—	Sucrose	99%	31%
SnO_2†	—	Sucrose	81%	4%

*Equivalent molar amount of Sn as for 160-mg Sn-Beta. †160 mg of SnO_2 used.

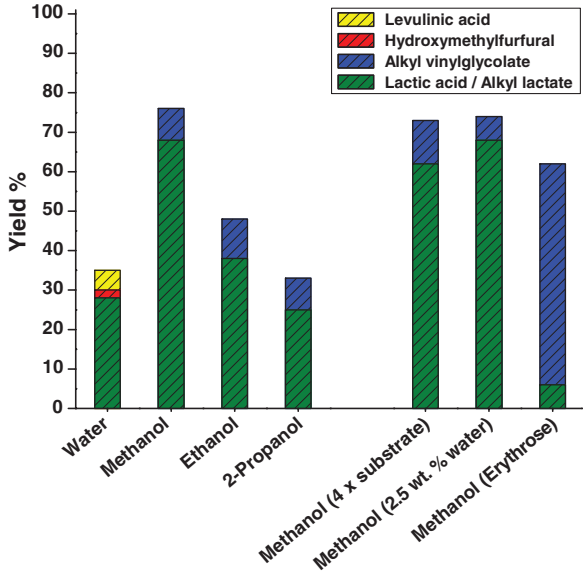

Fig. 2. Comparison of different solvents and reaction conditions for the conversion of sucrose using Sn-Beta (Si:Sn 165). Sucrose (225 mg), Sn-Beta (160 mg), and solvent (8.0 g) were stirred at 160°C for 20 hours.

the metals incorporated into the zeolite structure. Homogeneous $SnCl_4$ as well as nanocrystalline SnO_2, were also tested in the reaction. SnO_2 is inactive, whereas $SnCl_4$ shows moderate selectivity toward methyl lactate.

Glucose conversion proceeds in yields of methyl lactate comparable to those from fructose. We found that the Sn-Beta catalyst is capable of catalyzing Lobry-de Bruyn-van Ekenstein isomerization of glucose to fructose at low temperatures (100°C), which explains the similar yields obtained when using either of the hexoses. In addition, we observed that the disaccharide sucrose gives a substantially higher yield of methyl lactate as compared with fructose and glucose. This trend has also been observed for the alkaline degradation of fructose, glucose, and sucrose in water (*20*, *21*). This result is surprising, because the overall reaction pathway from sucrose to methyl lactate is thought to involve the intermediary formation of glucose and methyl fructoside by methanolysis, from which fructose is then formed via isomerization and hydrolysis, respectively (fig. S1).

Methyl lactate is not the only product formed during the reaction. The largest volatile coproduct is methyl vinylglycolate (methyl 2-hydroxy-3-butenoate), which is formed in yields ranging from 3 to 11% in all cases when using the Lewis acidic catalysts. Retro aldol reaction of glucose will produce erythrose (C_4 sugar) and glycolaldehyde (C_2). Methyl vinylglycolate formation could proceed by a reaction pathway analogous to that forming methyl lactate from trioses (fig. S1). To support this hypothesis, we heated D-erythrose to 160°C in methanol with Sn-Beta as the catalyst, and we observed methyl vinylglycolate formation in a considerably higher yield (56%) than that of methyl lactate (6%). Thus, tetroses appear to be precursors for methyl vinylglycolate (Fig. 2). Other products that were formed in small amounts from the mono- and disaccharides when using Sn-Beta are glycolaldehyde dimethylacetal (<1%), formaldehyde dimethylacetal (<1%), and methyl glycolate (<0.5%). Furthermore, we observed trace amounts of methyl 2-hydroxy butyrate and small amounts of methoxy derivatives of furfural and HMF (table S1 and fig. S2). Many of these products are similar to the saccharinic acids that are formed in the alkaline degradation of sugars, where major products are lactic acid, glycolic acid, 2,4-dihydroxybutanoic acid, as well as higher C_6 acids (*21*). In the case of Sn-Beta, we observed, using HPLC analysis, the presence of a noticeable amount of highly polar products, which could be methyl esters of the higher C_6 saccharinic acids. The combined yields of methyl lactate (68%) and methyl vinylglycolate (8%) exceed 75% for sucrose on a carbon basis when Sn-Beta (Si:Sn 165) is used as the catalyst. When the amount of sucrose and glucose is increased by a factor of four [>10 weight percent (wt %) in methanol], similar combined yields of methyl lactate and methyl vinylglycolate are obtained, and full conversion is still reached within 20 hours (Fig. 2). In this experiment, the average turnover number per Sn atom is >400 for the production of methyl lactate based on the assumed participation of all Sn atoms in the catalyst. A further increase in sucrose concentration to 20 wt % causes a drop in the yields of methyl lactate (47%) and methyl vinylglycolate (12%) in an experiment using twice the amount of Sn-Beta.

Changing the solvent from methanol to higher alcohols or water leads to the formation of the corresponding alkyl lactates and free lactic acid, respectively (Fig. 2 and see table S2 for data for glucose and fructose). Low amounts (<30%) of lactic acid are formed in water together with HMF (1 to 2%) and levulinic acid (~5%). Additionally, temperature-programmed oxidation showed that more carbon is deposited on the catalyst when water is used as the solvent (7.0 wt % of carbon per g catalyst) in place of methanol (1.3 wt %) (table S3). The change in the product composition when using water as the solvent can be explained by the auto-catalytic effect of the organic acids formed. Lactic acid and levulinic acid, being Brønsted acids, will shift the course of the reaction toward that typically seen with Brønsted acid catalysts (HMF, levulinic acid); the result is lower yields of the α-hydroxycarboxylic acid products formed in the pathway catalyzed by Lewis acids. Because small amounts of water are formed during the reaction, we examined the effect of water in methanol. Using a solvent mixture consisting of 2.5 wt % water in methanol, we obtained yields of methyl lactate similar to those obtained in pure methanol (Fig. 2). Changing the solvent to higher alcohols leads to a decrease in alkyl lactate selectivity. In ethanol, 39% of ethyl lactate is formed using sucrose as the substrate and Sn-Beta as the catalyst, whereas 25% of isopropyl lactate is formed in *i*-propyl alcohol.

Long-term stability is a very important characteristic for a heterogeneous catalyst. We therefore explored the prospects for reusing Sn-, Zr-, and Ti-Beta (Fig. 3). Each catalyst was used six times for the conversion of sucrose after calcining between each run to burn away deposited carbon. The catalysts were found to remain active with an almost unchanged selectivity even after the sixth reuse (fig. S5). After the fifth run, the zeotypes were calcined and analyzed by N_2-sorption and x-ray powder diffraction (XRPD) (fig. S6 and table S3). Analysis shows that the BEA structure is preserved and the micropore volumes for Ti-Beta and Zr-Beta remain constant; a very small volume decrease from 0.201 ml/g to 0.197 ml/g was observed for Sn-Beta. These data after >100 hours of catalyst use thus show promising stability characteristics. Further examination of the catalyst stability using a fixed bed reactor shows that Sn-Beta deactivates gradually as a function of time on stream (fig. S7). This indicates that the ability to regenerate the activity by calcination is an important feature of the catalyst. The reusability of Lewis acidic zeolites and zeotypes has also been reported in other reactions (*30*, *31*).

In contrast to the alkaline degradation, acid-catalyzed conversion of mono- and disaccharides does not consume a stoichiometric amount of base. However, the reaction pathway in the acid-catalyzed conversion is highly sensitive to the type of acid used. Whereas Brønsted acids catalyze monosaccharide dehydration reactions, leading primarily to HMF and its decomposition products, Lewis acidic zeotype catalysts lead to retro aldol reaction of the monosaccharides and subsequent transformation to α-hydroxycarboxylic acid derivatives. To achieve a high selectivity in the Lewis acid–catalyzed pathway, it is important to diminish the catalytic effect of Brønsted acids, for example, by using a solvent such as methanol in which esters, rather than free carboxylic acids, are formed.

Unlike the primary product of the Brønsted acid–catalyzed reaction, HMF, a market already exists for lactic acid and its ester derivatives. These compounds are now accessible from sucrose, glucose, and fructose, using non-noble metal–containing catalysts. However, the catalytic process results in a racemic product mixture. This plays no role for solvent or feedstock end-use, but enantiomeric purity is an important parameter in the production of biodegradable plastics.

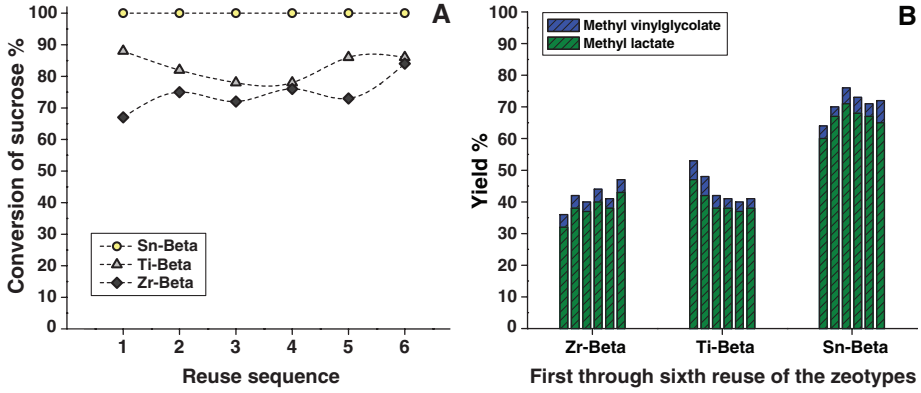

Fig. 3. Reuse of Sn-, Zr-, and Ti-Beta (Si/metal: 125) for the conversion of sucrose in methanol, with calcination of the zeotypes between each experiment. (**A**) Conversion of sucrose and (**B**) yields of methyl lactate and methyl vinylglycolate in the reuse experiments.

References and Notes

1. G. W. Huber, S. Iborra, A. Corma, *Chem. Rev.* **106**, 4044 (2006).
2. H. Danner, R. Braun, *Chem. Soc. Rev.* **28**, 395 (1999).
3. A. Corma, S. Iborra, A. Velty, *Chem. Rev.* **107**, 2411 (2007).
4. C. H. Christensen, J. Rass-Hansen, C. C. Marsden, E. Taarning, K. Egeblad, *Chem. Sus. Chem.* **1**, 283 (2008).
5. H. Zhao, J. E. Holladay, H. Brown, Z. C. Zhang, *Science* **316**, 1597 (2007).
6. Y. Román-Leshkov, J. N. Chheda, J. A. Dumesic, *Science* **312**, 1933 (2006).
7. M. Bicker, J. Hirth, H. Vogel, *Green Chem.* **5**, 280 (2003).
8. M. E. Himmel *et al.*, *Science* **315**, 804 (2007).
9. J. Lunt, *Polym. Degrad. Stabil.* **59**, 145 (1998).
10. E. T. H. Vink, K. R. Ràbago, D. A. Glassner, P. R. Gruber, *Polym. Degrad. Stabil.* **80**, 403 (2003).
11. K. L. Wasewar, A. A. Yawalkar, J. A. Moulijn, V. G. Pangarkar, *Ind. Eng. Chem. Res.* **43**, 5969 (2004).
12. R. Datta, M. Henry, *J. Chem. Technol. Biotechnol.* **81**, 1119 (2006).
13. Y. Fan, C. Zhou, X. Zhu, *Catal. Rev.* **51**, 293 (2009).
14. J. C. Serrano-Ruiz, J. A. Dumesic, *Chem. Sus. Chem* **2**, 581 (2009).
15. E. Taarning *et al.*, *Chem. Sus. Chem* **2**, 625 (2009).
16. R. M. West *et al.*, *J. Catal.* **269**, 122 (2010).
17. Y. Hayashi, Y. Sasaki, *Chem. Commun. (Camb.)* (21): 2716 (2005).
18. T. M. Aida *et al.*, *J. Supercrit. Fluid.* **42**, 110 (2007).
19. M. Sasaki, K. Goto, K. Tajima, T. Adschiri, K. Arai, *Green Chem.* **4**, 285 (2002).
20. R. Montgomery, *Ind. Eng. Chem.* **45**, 1144 (1953).
21. B. Y. Yang, R. Montgomery, *Carbohydr. Res.* **280**, 47 (1996).
22. G. Braun, U.S. patent 2,024,565 (1935).
23. Materials and methods are available as supporting material on *Science* Online.
24. J. M. Thomas, R. Raja, D. W. Lewis, *Angew. Chem. Int. Ed.* **44**, 6456 (2005).
25. M. Boronat, A. Corma, M. Renz, P. M. Viruela, *Chemistry* **12**, 7067 (2006).
26. A. Corma, *J. Catal.* **216**, 298 (2003).
27. J. Jow, G. L. Rorrer, M. C. Hawley, D. T. A. Lamport, *Biomass* **14**, 185 (1987).
28. P. Rivalier, J. Duhamet, C. Moreau, R. Durand, *Catal. Today* **24**, 165 (1995).
29. M. Renz *et al.*, *Chemistry* **8**, 4708 (2002).
30. J. C. van der Waal, E. J. Creyghton, P. J. Kunkeler, K. Tan, H. van Bekkum, *Top. Catal.* **4**, 261 (1997).
31. A. Corma, M. E. Domine, L. Nemeth, S. Valencia, *J. Am. Chem. Soc.* **124**, 3194 (2002).

32. The Catalysis for Sustainable Energy initiative is funded by the Danish Ministry of Science, Technology and Innovation. The Center for Sustainable and Green Chemistry is sponsored by the Danish National Research Foundation. Haldor Topsøe A/S holds patent application EP 090137829 related to the work described in this report. The authors thank C. Hviid Christensen (Haldor Topsøe A/S) for helpful advice.

Supporting Online Material

www.sciencemag.org/cgi/content/full/328/5978/602/DC1
Materials and Methods
Figs. S1 to S8
Tables S1 to S6
References

29 October 2009; accepted 17 March 2010
10.1126/science.1183990

Recent Hotspot Volcanism on Venus from VIRTIS Emissivity Data

Suzanne E. Smrekar,[1]* Ellen R. Stofan,[2] Nils Mueller,[3,6] Allan Treiman,[4] Linda Elkins-Tanton,[5] Joern Helbert,[6] Giuseppe Piccioni,[7] Pierre Drossart[8]

The questions of whether Venus is geologically active and how the planet has resurfaced over the past billion years have major implications for interior dynamics and climate change. Nine "hotspots"—areas analogous to Hawaii, with volcanism, broad topographic rises, and large positive gravity anomalies suggesting mantle plumes at depth—have been identified as possibly active. This study used variations in the thermal emissivity of the surface observed by the Visible and Infrared Thermal Imaging Spectrometer on the European Space Agency's Venus Express spacecraft to identify compositional differences in lava flows at three hotspots. The anomalies are interpreted as a lack of surface weathering. We estimate the flows to be younger than 2.5 million years and probably much younger, about 250,000 years or less, indicating that Venus is actively resurfacing.

Venus' resurfacing record holds important clues to its geological evolution. Venus and Earth are similar in size and in internal heat production, yet Venus is in a stagnant lid convection regime whereas Earth has vigorous plate tectonics. Venus' sparse and largely unmodified crater population has spawned a debate over whether it was resurfaced catastrophically (*1*) or gradually (*2*). These two end members have very different dynamic implications. Catastrophic resurfacing could have been caused by episodic mantle overturn (*3*) or melting in a hot mantle insulated by a stagnant lid (*4*). Gradual resurfacing is consistent with more Earth-like volcanic and interior processes (*5*). The rate and style of resurfacing have important implications for both interior evolution and climate change driven by volatile release from volcanic outgassing.

The Visible and Infrared Thermal Imaging Spectrometer (VIRTIS) on the European Space Agency's Venus Express spacecraft provided a map of thermal emission for much of the southern hemisphere of Venus' surface in the atmospheric window at 1.02 μm (*6*). Surface emissivities in the 1.02-μm band are retrieved from surface brightness by correcting for effects of instrumental stray light, viewing geometry, cloud opacity, and elevation (*7*, *8*). More accurate topographic data (*9*) allowed us to make significantly better maps of surface emissivity (*10*). Absolute surface emissivities are model-dependent (*11*) but are calculated from variations in the emitted fluxes that are up to 12% greater than the average value. These emissivity variations represent differences in material

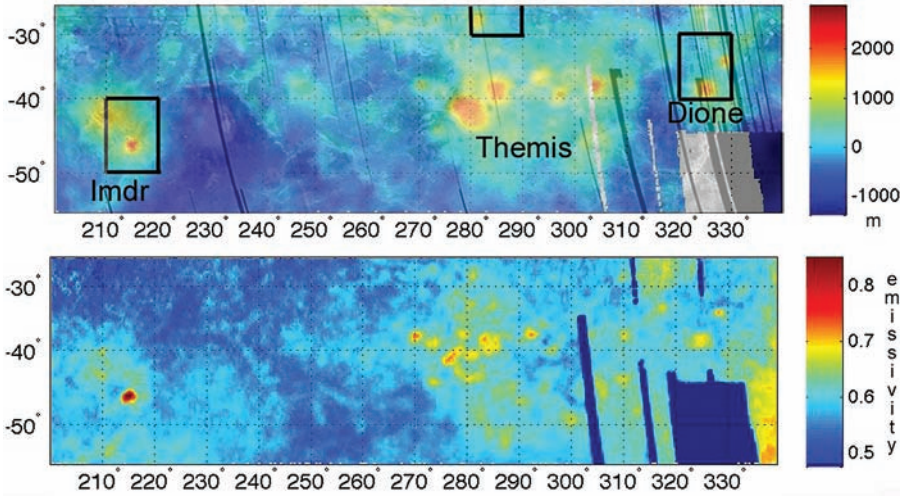

Fig. 1. (**Top**) Magellan synthetic aperture radar (SAR) image, left looking, overlain on topography. (**Bottom**) Surface emissivity derived from the VIRTIS spectrometer. Regio names are located below the topographic rises. Boxes indicate example sites shown in Fig. 2.

[1]Jet Propulsion Laboratory, Mail Stop 183-501, 4800 Oak Grove Drive, Pasadena, CA 91109, USA. [2]Proxemy Research, 20528 Farcroft Lane, Laytonsville, MD 20882, USA. [3]Institute for Planetology, Westfälische Wilhelms-Universität Münster, Wilhelm-Klemm-Strasse 10, 48149 Münster, Germany. [4]Lunar and Planetary Institute, 3600 Bay Area Boulevard, Houston, TX 77058, USA. [5]Massachusetts Institute of Technology, Earth, Atmospheric, and Planetary Sciences, Building 54-824, 77 Massachusetts Avenue, Cambridge, MA 02139, USA. [6]Institute of Planetary Research, German Aerospace Center, Rutherfordstrasse 2, D-12489 Berlin, Germany. [7]Istituto Nazionale di Astrofisica–Istituto di Astrofisica Spaziale e Fisica Cosmica (INAF-IASF), Via del Fosso del Cavaliere 100, 00133 Rome, Italy. [8]Laboratoire d'Etudes Spatiales et d'Instrumentation en Astrophysique (LESIA), Observatoire de Paris, CNRS, UPMC, Université Paris-Diderot, 5 Place Jules Janssen, 92195 Meudon, France.

*To whom correspondence should be addressed. E-mail: ssmrekar@jpl.nasa.gov